Makara Journal of Science

Volume 24
Issue 4 *December*

Article 7

12-20-2020

Computational Analysis of Chromophore Tripeptides FollowingFusion of Enhanced Green Fluorescent Protein and Cell-penetrating Peptides

Silvia Tri Widyaningtyas
Virology and Cancer Pathobiology Research Centre, Faculty of Medicine, Universitas Indonesia - Dr Cipto Mangunkusumo General Hospital, Jakarta, Indonesia, silvia.widyaningtyas@ui.ac.id

Ekawati Betty Pratiwi
Virology and Cancer Pathobiology Research Centre, Faculty of Medicine, Universitas Indonesia - Dr Cipto Mangunkusumo General Hospital, Jakarta, Indonesia

Budiman Bela
Department of Clinical Microbiology, Faculty of Medicine, Universitas Indonesia - Dr. Cipto Mangunkusumo General Hospital, Jakarta, Indonesia

Makara Journal of Science, 24/4 (2020), 249–256
doi: 10.7454/mss.v24i4.1213

Computational Analysis of Chromophore Tripeptides FollowingFusion of Enhanced Green Fluorescent Protein and Cell-penetrating Peptides

Silvia Tri Widyaningtyas[1*], Ekawati Betty Pratiwi[1], and Budiman Bela[1,2]

1. Virology and Cancer Pathobiology Research Centre, Faculty of Medicine, Universitas Indonesia - Dr Cipto Mangunkusumo General Hospital, Jakarta 10430, Indonesia
2. Department of Clinical Microbiology, Faculty of Medicine, Universitas Indonesia - Dr. Cipto Mangunkusumo General Hospital, Jakarta 10430, Indonesia

[*]*E-mail: silvia.widyaningtyas@ui.ac.id*

Received October 8, 2019 | Accepted September 3, 2020

Abstract

Cell-penetrating peptides (CPPs) are small peptides that can transfer other materials into a cellular compartment. In this research, we studied the effect of fusion of new CPPs to the N-terminal of enhanced Green Fluorescent Protein eGFP on the ability of the latter to fluoresce. Results showed that the recombinant protein CPPs-eGFP could be successfully expressed in *Escherichia coli*. In contrast to *E. coli* expressing wild-type eGFP, which could fluoresce under ultraviolet (UV) or visible light, *E. coli* expressing CPPs-eGFP lost their ability to fluoresce. PyMol, a molecular visualization system, revealed that fusion of the new CPPs to the N-terminal of eGFP alters interactions between chromophore-forming tripeptides and the adjacent amino acids of other tripeptides. Disrupting peptide interactions induced structural changes in eGFP that caused it to lose its fluorescence ability. We suggest performing computational analyses to predict the biological function of new fusion proteins prior to starting laboratory work.

Keywords: ALMR, CPP, eGFP, SIMR

Introduction

The successful delivery of a material, especially one used for gene therapy, DNA/mRNA vaccination, genome editing, and many other biological applications, into the intracellular compartment is an important endeavor [1]. Viral vectors are the most well-developed vehicles used to deliver extracellular materials. The use of viral vectors ensures that the extracellular material is effectively distributed into the intracellular compartment. However, these vectors may also induce an immune response that could affect its transport efficiency. Some viral vectors may even cause severe side effects. To overcome those obstacles, researchers over the last 20 years have sought to develop vehicles based on small peptides. The first peptide to deliver a material larger than itself is one derived from trans-activator of transcription (Tat) protein, a human immunodeficiency virus accessory protein [2]. Small peptides that can transfer other materials into a cellular compartment are called cell-penetrating peptides (CPPs) [3].

In vitro and in vivo studies have demonstrated the obstacles that must be overcome by CPPs. The presence of protease in the plasma, cell membrane, endosomal environment, and nuclear membrane could hinder the effectiveness of CPPs in delivering their cargo to the intracellular compartment [4]. Newer CPPs have been developed to avoid such issues [5,6]. These CPPs, such as ALMR and SIMR, are designed to deliver nucleic acids into the nucleus of non-dividing cells [5,6]. In a previous study, these CPPs protected DNA from plasma-nuclease degradation, delivered DNA across the membrane cells, escaped from the endosomal compartment, and crossed the nuclear membrane [6]. The ability of these new CPPs to deliver protein cargos into the intracellular compartment must be investigated further. The discovery of CPPs that can deliver proteins or molecules into an intracellular environment provides new opportunities for the development of medical treatment using proteins or molecules previously considered incompatible for therapy [7,8].

Proteins may be incorporated into CPPs via their fusion and expression in a suitable system, such as prokaryotes [9]. A previous study reported the ability of prokaryotic expression systems to express CPPs fused to many reporter proteins, such as GFP [10]. Fusion of CPPs to the C or N-terminal of a protein could alter the structure and biological function of the latter [11]. In this research, we studied the effect of fusing ALMR and

SIMR to the N-terminal of eGFP on the ability of the latter to fluoresce. Analyses of the *Escherichia coli* expression, biological properties, and structures of the resulting proteins were also performed.

Material and Methods

Plasmids coding ALMR-eGFP, SIMR-eGFP, and eGFP protein. pQEALMR-eGFP, pQESIMR-eGFP, and pQEeGFP coding ALMR-eGFP, SIMR-eGFP, and eGFP protein, respectively, were obtained from VCPRC FKUI-RSCM. Genes coding ALMR-eGFP, SIMR-eGFP, and eGFP were inserted downstream of the 6×histidine tag. Recombinant proteins were tagged with 6×histidine to promote their purification using NiNTA immobilized-metal affinity chromatography (IMAC).

Protein expression. ALMR-eGFP and eGFP were expressed in *E. coli* DH5α, and SIMR-eGFP was expressed in *E. coli* BL21 [Novagen]. Protein expression was conducted using the method described in QIAexpressionist [12]. One bacterial colony was grown in LB broth media [HiMedia] containing 100 μg/ml ampicillin. After overnight incubation at 37 °C, the starter culture was used to inoculate a larger volume of Terrific broth containing 100 μg/ml ampicillin at a 1:10 ratio. After 2 hours of incubation at 37 °C, IPTG was added to the bacterial cultures at a final concentration of 1 mM. The cultures were incubated for another 4 hours, and the GFP fluorescence of the bacterial pellets was observed by direct visualization with the naked eye and short-wave UV light. ALMR-eGFP, SIMR-eGFP, and eGFP were analyzed using SDS-PAGE.

Bacterial lysis. Bacteria expressing eGFP proteins were lysed under native conditions following the methods described in QIAexpressionist [1210]. The bacterial pellet was diluted in native buffer (50 mM NaH_2PO_4 [Applichem], 300 mM NaCl, 10 mM imidazole, pH 8), and the bacterial suspension was sonicated over six cycles of bursting; each burst lasted 20 seconds, and the interval between bursts was 10 seconds. After sonication, the bacterial suspension was centrifuged at 8000 rpm for 30 minutes at 4 °C. The supernatant was stored at −30 °C. Bacteria expressing ALMR-eGFP and SIMR-eGFP were lysed under denaturing conditions by using denaturant buffer (100 mM NaH_2PO_4 [Applichem], 10 mM TrisCl [Thermo Scientific], 6 M guanidine hydrochloride [Bio Basic Inc. pH 8) [13]. After incubation in a rotary shaker for 1 hour at room temperature, the bacteria were centrifuged at 8000 rpm for 30 minutes at 4 °C to separate proteins and cell debris. The supernatant was stored at −30 °C.

Protein purification. Recombinant proteins were purified by IMAC according to the principles of histidine–NiNTA binding [14] by using a commercial kit from Qiagen. Purification was conducted as described by the manufacturer. Recombinant proteins were desalted using PD10 columns (GE Healthcare) following the manufacturer's recommendation.

Western blot analysis. Western blot analysis was conducted following the methods described by Ni *et al.* [15]. The proteins obtained by SDS-PAGE were transferred to a nitrocellulose membrane, which was subsequently blocked with 1% skim milk (BioRad) and incubated in PBS-diluted primary antibody (rabbit polyclonal antibody against GFP; VPRVC FKUI) at a 1:10 ratio (v/v) at room temperature. The membrane was washed thrice with PBS–Tween and then added with the secondary antibody (biotinylated anti-rabbit IgG). Following the washing steps described above, the membrane was incubated with streptavidin HRP for 1 hour at room temperature and washed thrice with PBS. Protein bands were visualized by adding Immunostar chemiluminescent substrate (Invitrogen) to the membrane. Western blot bands were captured using an LA 4000 instrument (Thermo Scientific).

Protein structure analysis. RaptorX software was used to obtain the tertiary structure and 3D model of the proteins [16]. PyMOL Molecular Graphics System version 1.7.x was used to visualize the predicted structures of the proteins [17].

Result and Discussion

DH5α pellets expressing ALMR-eGFP did not show fluorescence under visible or UV light (Figure 1.A.2 and 1.B.2). The same result was observed in BL21 expressing SIMR-eGFP (Figure 1.C.2 and 1.D.2). By contrast, the fluorescence of DH5α and BL21expressing eGFP could be observed under visible and UV light (Figure 1.A.3, 1.B.3, 1.C.2, and 1.D.3). The fluorescence of control DH5α and BL21 cells was not observed under visible (Figure 1.A.1 and Figure 1 C.1) or UV (Figure 1.C.1 and 1.D.1) light. The inability of bacteria expressing ALMR-eGFP or SIMR-eGFP to fluoresce may be related to the inability of the same to produce ALMR-eGFP and SIMR-eGFP. Thus, SDS-PAGE analyses were performed to confirm the expression of our proteins of interest.

SDS-PAGE analyses revealed the overexpression of protein bands measuring 32, 31, and 27 kDa in size, which were correlated with ALMR-eGFP, SIMR-eGFP, and eGFP respectively. These results indicate the absence of obstacles preventing bacteria from producing ALMR-eGFP and SIMR-eGFP (Figure 2).

NiNTA chromatography purification could produce a pure recombinant protein that is free of any bacterial protein contamination. Purified ALMR-eGFP and SIMR-eGFP could be used for further in vitro studies. eGFP purification was performed under native

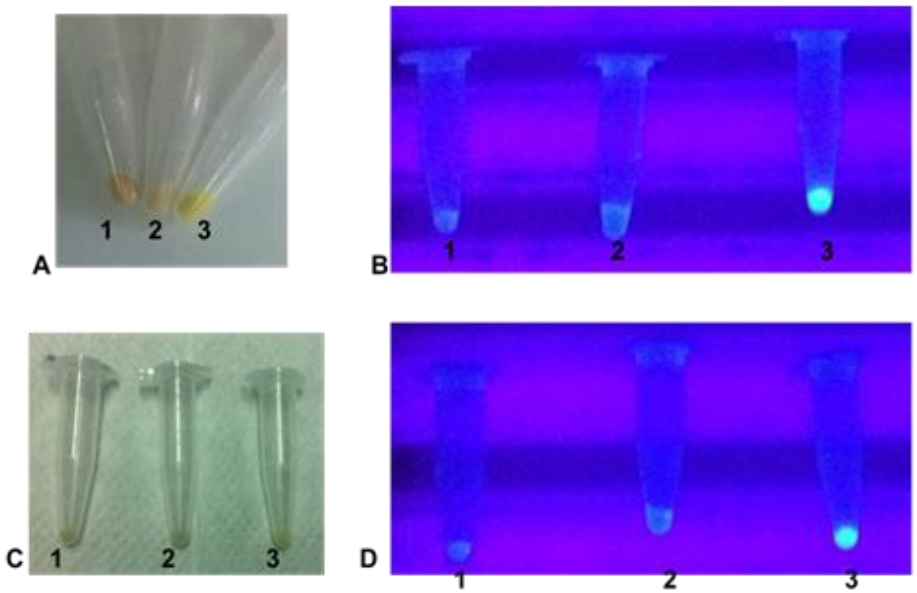

Figure 1. Bacterial Pellet Expressing ALMR-eGFP, SIMR-eGFP, and eGFP Proteins. (A) Bacterial Pellet under Visible Light. 1. DH5α, 2. DH5α Expressing ALMR-eGFP, and 3. DH5α Expressing eGFP. (B) Bacterial Pellet under Ultraviolet Light. 1. DH5α, 2. DH5α Expressing ALMR-eGFP, and 3. DH5α Expressing eGFP. (C) BL21 Expressing SIMR-eGFP Under Visible Light. 1. BL21, 2. BL21 Expressing ALMR-eGFP, and 3. BL21 Expressing eGFP. (D) BL21 Expressing SIMR-eGFP under UV light. 1. BL21, 2. BL21 Expressing ALMR-eGFP, and 3. BL21 Expressing eGFP

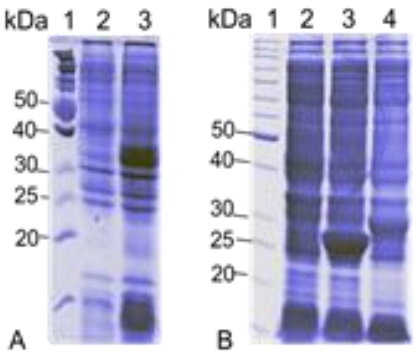

Figure 2. SDS-PAGE Analysis of ALMR-eGFP, SIMR-eGFP, and eGFP WT. (A) ALMR-eGFP. Lane 1, marker; Lane 2, Uninduced Bacteria; Lane 3, ALMR-eGFP (32 kDa). (B) SIMR-eGFP Expression. Lane 1, Marker; Lane 2, Uninduced Bacteria; Lane 3, eGFP (27 kDa); Lane 4, SIMR-eGFP (31 kDa)

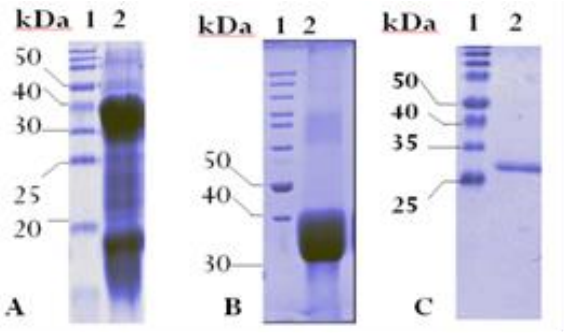

Figure 3. Purified (A) ALMR-eGFP (32 kDa), (B) SIMR-eGFP (31 kDa), and (C) eGFP (27 kDa)

conditions, but neither ALMR-eGFP nor SIMR-eGFP could be purified (unpublished data). This finding may be attributed to the burial of 6×histidine in these proteins. Purification of ALMR-eGFP and SIMR-eGFP was performed under denaturing conditions (Figure 3). However, nonspecific bands could be observed in the purified-ALMR-eGFP and SIMR-eGFP (Figure 3A). Purified-eGFP (Figures 3B and 3C) did not show nonspecific bands.

Western blot analysis was used to verify the recombinant proteins on the basis of their reactivity to a specific antibody. The results showed that ALMR-eGFP, SIMR-eGFP, and eGFP react to rabbit polyclonal antibody against eGFP. In these proteins, the polyclonal antibody reacted with only a single band protein, which indicates that nonspecific proteins copurified by NiNTA are not reactive to antibodies against GFP (Figure 4).

PyMol revealed that ALMR-eGFP and SIMR-eGFP have structures resembling that of eGFP (Figure 5). eGFP has a unique barrel shape formed by 11 β-sheets and a coaxial α-helix traversing the center of the β-barrel. Differences in the diameters of the β-barrels of ALMR-eGFP, SIMR-eGFP, and eGFP were observed.

The diameters of the β-barrels of ALMR-eGFP, SIMR-eGFP and eGFP were 19.7, 19.3, and 19.4 Å, respectively. The structure of the tripeptide in ALMR-eGFP is different from those in SIMR-eGFP and eGFP. Specifically, the tripeptide in ALMR-eGFP forms a loop structure whereas the tripeptides in SIMR-eGFP and eGFP WT form an α-helical structure (Figures 5a and 5b).

The interactions of tripeptides with adjacent amino acids and the orientation of some amino acids in ALMR-eGFP and SIMR-eGFP differed from those in eGFP. In eGFP, Ser^{65} and Tyr^{66} interact with His^{148} and Glu^{222}, which are located on β-sheets, while Gly^{67} interacts with Gln^{94} and Arg^{96}, which are also located on β-sheets (Figure 6 A.1.). The imidazole ring of His^{148} in eGFP points toward the tripeptide. By contrast, the imidazole ring of His^{148} in ALMR-eGFP points outward from the β-barrel wall (Figure 6 A.2). Changes in His^{148} orientation widen the distance between His^{148} and Tyr^{66} and weaken the interaction between these two amino acids (Figure 6.A.2). In ALMR-eGFP, no interactions between Ser^{65} and Tyr^{66} with His^{148} and Glu^{222} and between Gly^{67} with Gln^{94} and Arg^{96} occur (Figure 6.A.2). In SIMR-eGFP, the interactions of His^{148} with Ser^{65}, Tyr^{66}, and Glu^{222}, as well as that of Gly^{67} and Arg^{96}, are weak (Figure 6.C.1.). The distance between Tyr^{66} and Glu^{222} in SIMR-eGFP (6.2 Å) is smaller than that in eGFP (6.5 Å) (Figure 6.B.1 and Figure 6). Similarly, the distance between Thr^{65} and Tyr^{66} in SIMR-eGFP (7.9 Å) is smaller than that in eGFP (8.2 Å) (Figures 6.B.1 and 6.B.2). Using PyMol, we found a cavity in the SIMR-eGFP β-barrel structure causing the exposure of tripeptides, i.e., Tyr^{66} and Thr^{65}, as well as an adjacent amino acid, i.e., Glu222 (Figure 6.C.2), to the environment (Figure 6.C.2). The tripeptide of eGFP was protected inside the β-barrel structure (Figure 6.C.1).

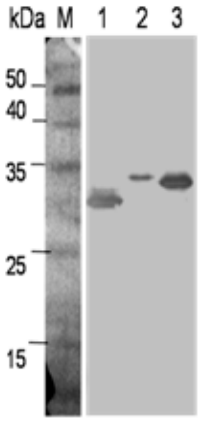

Figure 4. Reactivity of the GFP Antibody to Purified Recombinant Proteins. ALMR-eGFP, SIMR-eGFP, and eGFP were Reactive to Anti-eGFP. Line 1, eGFP (27 kDa); Line 2, ALMR-eGFP (32 kDa); Line 3, SIMR-eGFP (31 kDa)

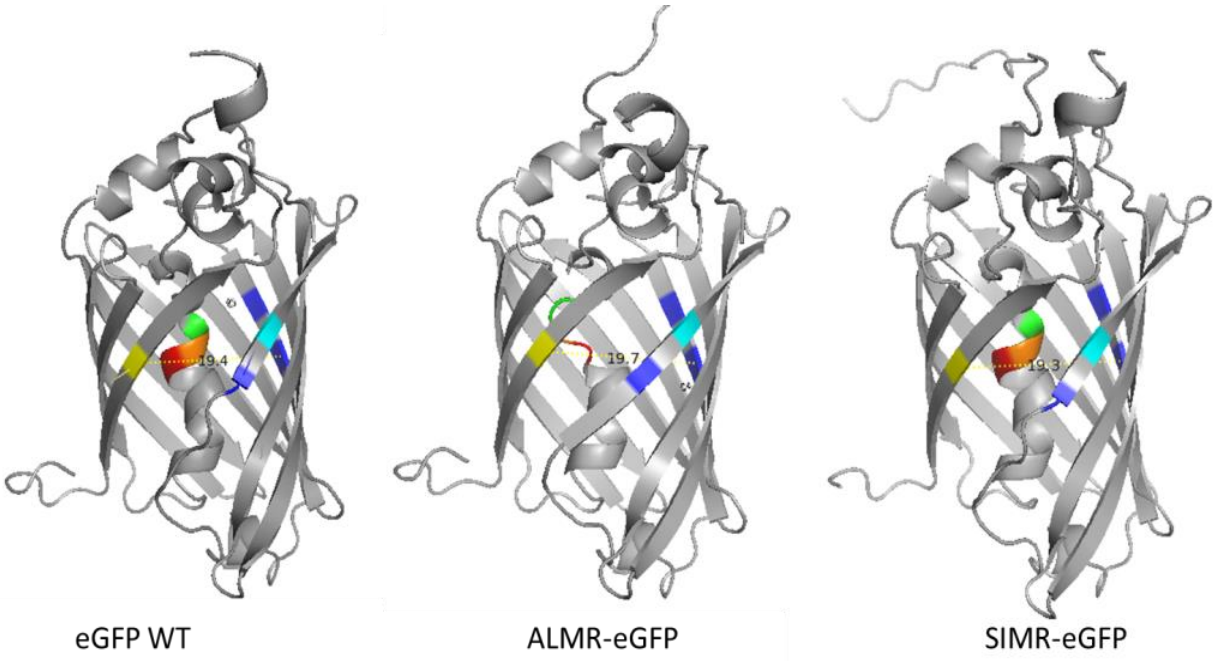

Figure 5. Barrel Structures of eGFP, ALMR-eGFP, and SIMR-eGFP. The Tripeptide Ser^{65}-Tyr^{66}-Gly^{67} is Indicated in Red, Yellow, and Green at the Center of the β-barrel. Blue Indicates Amino Acids Interacting with Ser^{65}-Tyr^{66}-Gly^{67}. Yellow and Cyan Represent Adjacent Amino Acids Interacting with Ser^{65}-Tyr^{66}-Gly^{67} after Fusion with ALMR or SIMR

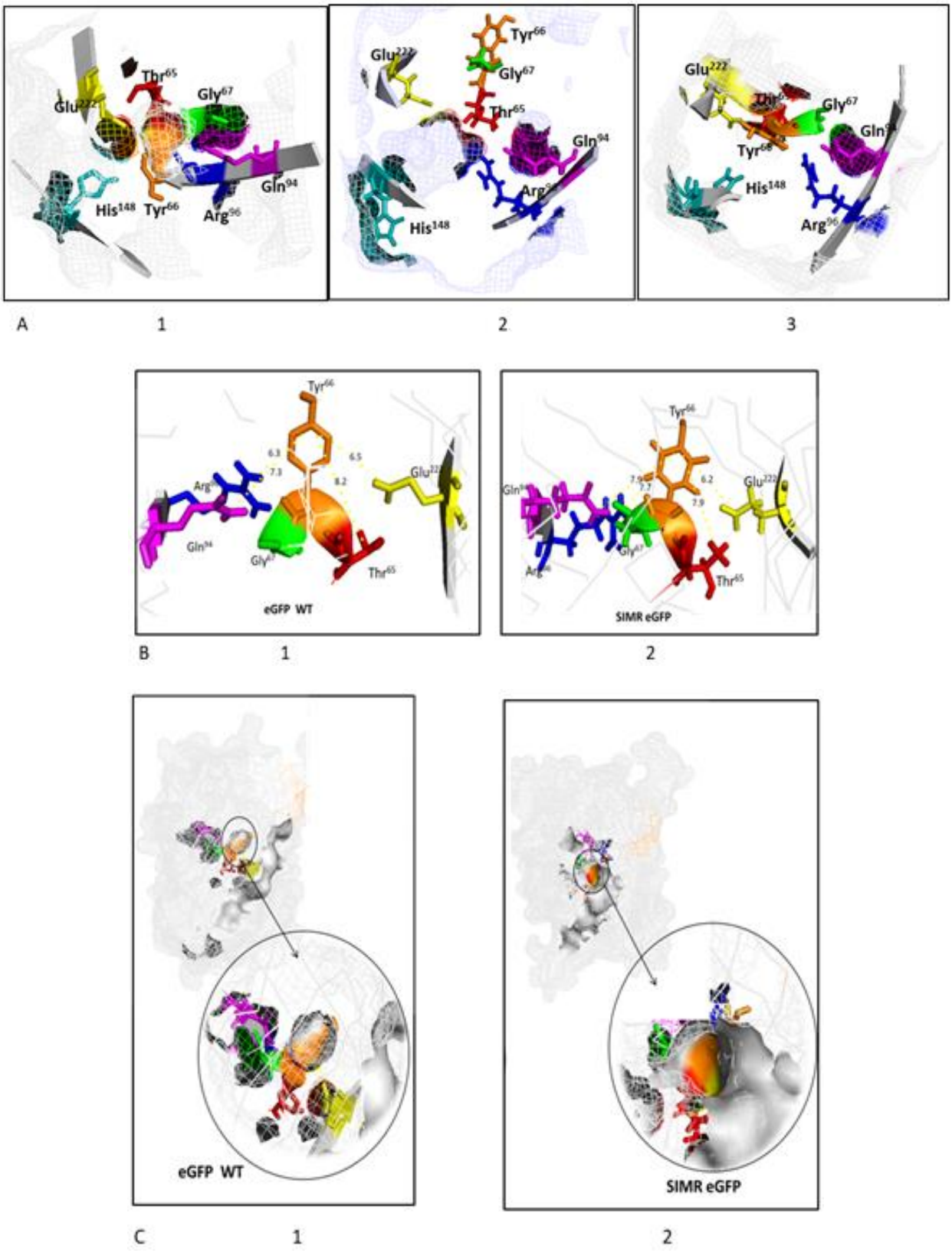

Figure 6. Tripeptide and Adjacent Amino Acids Determining the Fluoresce of GFP. (A) Interaction of the Tripeptide with Adjacent Amino Acids. (B) Proximity of Tyr^{66} to Glu^{222} and Thr^{65} in eGFP and SIMR-eGFP. (C) Cavity Formation in SIMR-eGFP

ALMR and SIMR are new CPPs that bind and deliver DNA into the nucleus of dividing and non-dividing cells [5,6]. The ability of these CPPs to deliver extracellular proteins to intracellular compartments remains debated. In this study, we fused ALMR and SIMR to the N-terminal of eGFP. GFP and its variants are reporter proteins widely used to study biological processes in many species [18,19]. In this study, we found that fusion with ALMR and SIMR alters the GFP structure and causes it to lose its ability to fluoresce.

All of the proteins used in this study were fused to 6×histidine to assist in their purification. Addition of 6×histidine alone to the N-terminal of eGFP does not alter GFP fluorescence (Figure 1). This finding is consistent with the results of Deng and Boxer in 2020 [20]. Purification of ALMR-eGFP and SIMR-eGFP was performed under denaturing conditions in which eGFP may be unable to fluoresce. Thus, the proteins were desalted using a PD10 column to reduce the effects of the denaturant. The diluted denaturant in solution did not affect the fluorescence of ALMR-eGFP and SIMR-eGFP. This finding indicates that the structures of AMLR-eGFP and SIMR-eGFP had changed during their expression in *E. coli*.

PyMol computational analysis allowed the intensive study of the structures of ALMR and SIMR upon fusion with eGFP. Fusion of ALMR and SIMR to the N-terminal of eGFP did not affect the formation of 11 β-sheets and a central coaxial helix to build a cylindrical β-barrel structure resembling that of eGFP [21]. However, this fusion induced changes in the structure of the latter that caused it to lose its fluorescence.

The chromophore tripeptide, which comprises amino acid numbers 65–67, of *Aequorea victoria*'s GFP plays an important role in its fluorescence [24]. Many proteins in nature contain the tripeptide sequence, but most of them cannot fluoresce. This finding highlights the crucial role of other amino acids in the generation of chromophores [20,21]. Some studies have demonstrated the role of the interaction of tripeptides with adjacent and remote amino acids from other tripeptides in the formation of chromophores [24,25]. A limitation of our study is that our computational analysis focuses on interactions between the amino acids of a tripeptide and those of another adjacent tripeptide. Alterations in these interactions affect GFP fluorescence [24].

The tripeptide $Thr^{65}Tyr^{66}Gly^{67}$ is located at the α-helix at the center of the β-barrel structure [20]. This rigid β-barrel structure makes up a protein matrix that surrounds the tripeptide [24,26,27], protects it from nonradiative deactivation by oxygen and light in the environment, and ensures its flexibility [22,26,27]. In ALMR-eGFP, the structure of the tripeptide changes from α-helical to β-sheets. This change affects the interaction between a chromophore-forming tripeptide and its adjacent amino acids. Glycine has a H atom on its side chain that confers it with flexibility [29]. The interaction of Gly^{67} with Thr^{65} forms a kinked internal α-helix that places Gly^{67} close to Thr^{65} for nucleophilic attack during chromophore synthesis [25]. In ALMR-eGFP, Gly^{67} lose its interaction with Thr^{65}. The interaction of Glu^{222} and Thr^{65} determines the ability of GFP to adsorb light at 400 nm [20]. This crucial interaction is found in ALMR-eGFP; thus, ALMR-eGFP can absorb light at 400 nm but fails to emit light or synthesize chromophores at 509 nm. The proximity of backbone atoms in Thr^{65} and Tyr^{66} determines the cyclization of the imidazole ring, which is a critical step in eGFP fluorescence [23]. Changing the orientation of His^{148} in the imidazole ring in ALMR-eGFP abolishes the His^{148}–Tyr^{66} interaction. The anionic interaction between His^{148} and Try^{66} stabilizes the interactions of the tripeptide with crucial amino acids, namely, Gln^{94}, Arg^{96}, and Glu^{222}, in adjacent tripeptides [23]. Loss of this interaction in ALMR-eGFP destabilizes the tripeptide orientation and structure.

Fusion of SIMR to the N-terminal of eGFP triggers the formation of a cavity that leaves the tripeptide directly exposed to oxygen and light in the environment.. The fluorescence of GFP begins with the folding of the protein, which promotes the cyclization of Thr^{65} and Gly^{67}. This process induces the formation of an imidazoline-5-one intermediate structure followed by low oxygenation of the Tyr^{66} side chains [25,30]. However, excess oxygen causes photobleaching of the protein [25]. SIMR-eGFP may absorb light at 400 nm because of the occurrence of Glu^{222} and Thr65 interactions. In SIMR-eGFP, the chromophore is formed, but excessive exposure to light and oxygen causes GFP photobleaching. SIMR-eGFP also shows a loss of the His^{148}–Tyr^{66} interaction, which stabilizes the interaction of the tripeptide with the adjacent amino acids of other tripeptides.

Conclusion

Using PyMol, we found that fusion of ALMR and SIMR to the N-terminal of eGFP induces structural changes in the latter and renders it unable to fluoresce. We recommend performing predictions of the biological function of a new fusion protein by using computational analysis prior to starting laboratory work to produce recombinants.

Acknowledgements

This project was supported by the National Institute of Health Research and Development, Indonesian Ministry of Health, through Risbin Iptekdok.

Author Contributions

S.T.W. and E.B.P. acquired funding for this work, S.T.W. and E.B.P. performed the experiments, S.T.W. analyzed the data, and S.T.W. and B.B. wrote the paper.

References

[1] Stewart, M.P., Sharei, A., Ding, X., Sahay, G., Langer, R., Jensen, K.F. 2016. In vitro and ex vivo strategies for intracellular delivery. Nat. 538(7624): 183–192, http://dx.doi.org/10.1038/nature19764.

[2] Green, M., Ishino, M., Loewenstein, P.M. 1989. Mutational analysis of HIV-1 Tat minimal domain peptides: Identification of trans-dominant mutants that suppress HIV-LTR-driven gene expression. Cell. 58: 215–223, http://dx.doi.org/10.1016/0092-8674(89)90417-0.

[3] Tabujew, I., Lelle, M., Peneva, K. 2015. Cell-penetrating peptides for nanomedicine–how to choose the right peptide. BioNanoMaterials, 16(1). http://dx.doi.org/10.1515/bnm-2015-0001.

[4] Derakhshankhah, H., Jafari, S. 2018. Cell-penetrating peptides: A concise review with emphasis on biomedical applications. Biomed. Pharmacother. 108: 1090–1096, http://dx.doi.org/10.1016/j.biopha.2018.09.097.

[5] Widyaningtyas, S.T., Soebandrio, A., Ibrahim, F., Bela, B. 2017. Design, synthesis, and functional testing of recombinant cell-penetrating peptides. J. Phys. Conf. Ser. 884: 012030, http://dx.doi.org/10.1088/1742-6596/884/1/012030.

[6] Widyaningtyas, S.T. 2016. Pengembangan penghantar DNA berbasis polipeptida sebagai upaya meningkatkan efisiensi dan efektivitas transfeksi DNA pada sel mamalia (Development Peptide-mediated DNA delivery system to increase the effiiency dan effectiveness of DNA transfection into mammalian cells) (2016). [Disertasi]. Universitas Indonesia.

[7] Dinca, A., Chien, W.M., Chin, M.T. 2016. Intracellular Delivery of Proteins with Cell-Penetrating Peptides for Therapeutic Uses in Human Disease. Int. J. Mol. Sci. 17(2): 263, http://dx.doi.org/10.3390/ijms17020263

[8] Seo, B.J., Hong, Y.J., Do, J.T. 2017. Cellular Reprogramming Using Protein and Cell-Penetrating Peptides. Int. J. Mol. Sci. 18(3): 552, http://dx.doi.org/10.3390/ijms18030552.

[9] Sayanee, A.T.I., Alahmadib, Z.G., Amy, J.K. 2018. Expression of Cell-Penetrating Peptides Fused to Protein Cargo. J. Mol. Microbiol. Biotechnol. 28(15): 9–168, http://dx.doi.org/10.1159/000494084.

[10] Dey, C., Narayan, G., Kumar, H.K., Borgohain, M.P., Lenka, N., Thummer, R.P. 2017. Cell-penetrating Peptides as a Tool to Deliver Biologically Active Recombinant Proteins to Generate Transgene-free Induced Pluripotent Stem Cells. Stud. Stem. Cells Res. Ther. 3(1): 006–015, http://dx.doi.org/10.17352/sscrt.000011.

[11] Miller, S.E., Schneider, J.P. 2019. The effect of turn residues on the folding and cell-penetrating activity of β-hairpin peptides and applications toward protein delivery. Pept. Sci. e24125, http://dx.doi.org/10.1002/pep2.24125.

[12] The QIAexpressionist ™. 2003. A handbook for high-level expression and purification of 6xHis-tagged proteins. 4TH ed. Qiagen.

[13] Sigh, S.M., Panda, A,K. 2005. Solubilization and Refolding of Bacterial Inclusion Body Proteins. J. Biosci. Bioeng. 99(4): 303–310, http://dx.doi.org/10.1263/jbb.99.303.

[14] Bornhorst, J.A., Falke, J.J. 2000. Purification of proteins using polyhistidine affinity tags. Methods Enzymol. 326: 245–254, http://dx.doi.org/10.1016/s0076-6879(00)26058-8.

[15] Ni, D., Xu, P., Gallagher, S. 2016. Immunoblotting and Immunodetection. Curr. Protocols Mol. Biol. 10.8,1–10.8.37, http://dx.doi.org/10.1002/0471142727.mb1008s114.

[16] Källberg, M., Wang, H., Wang, S., Peng, J., Wang, Z., Lu, H., Xu, J. 2012. Template-based protein structure modeling using the RaptorX web server. Nat. Protocols 7. 1511–1522, http://dx.doi.org/10.1038/nprot.2012.085.

[17] Delano, W.L. The PyMOL Molecular Graphics System. 2002. Delano Scientific, San Carlos, CA, USA.

[18] Chudakov, D.M., Matz, M.V., Lukyanov, S., Lukyanov, K.A. 2010. Fluorescent proteins and their applications in imaging living cells and tissues. Physiol. Rev. 90: 1103–1163, http://dx.doi.org/10.1152/physrev.00038.2009.

[19] Day, R.N., Davidson, M.W. 2009. The fluorescent protein palette: tools for cellular imaging. Chem. Soc. Rev. 38(10): 2887–2921, http://dx.doi.org/10.1039/b901966a.

[20] Deng, A. Boxer, S.G. 2018. Structural Insight into the Photochemistry of Split Green Fluorescent Proteins: A Unique Role for a His-Tag. J. Am. Chem. Soc. 140(1): 375–381, http://dx.doi.org/10.1021/jacs.7b1.

[21] Ormö, M., Cubitt, A.B., Kallio,K., Gross, L.A., Tsien, R.Y., Remington. S.J. 1996. Crystal structure of the Aequorea victoria green fluorescent protein. Sci. 273: 1392–1395, http://dx.doi.org/10.1126/science.273.5280.1392.

[22] Stepanenko, O., Stepanenko, O., Shcherbakova, D., Kuznetsova, I., Turoverov, K., Verkhusha, V. 2011. Modern fluorescent proteins: from chromophore formation to novel intracellular applications. BioTechniques. 51(5), http://dx.doi.org/10.2144/000113765.

[23] Philip Jr. G.N.1997. Structure and dynamics of green fluorescent protein. Curr. Opin. Struct. Biol.

7(6): 821–7, http://dx.doi.org/10.1016/s0959-440x(97)80153-4.
[24] Yang, F., Moss, L.G., Phillips Jr. G.N. 1996. The molecular structure of the green fluorescent protein. Nat. Biotechnol. 14: 1246–1251, http://dx.doi.org/10.1038/nbt1096-1246.
[25] Pakhomov, A.A, Martynov, V.I. GFP family: structural insights into spectral tuning.2008. Chem. Biol. 15: 755–764, http://dx.doi.org/10.1016/j.chembiol.2008.07.009.
[26] Remington, S.J. 2006. Fluorescent proteins: maturation, photochemistry, and photo-physics. Curr. Opin. Struct. Biol. 16: 714–721, http://dx.doi.org/10.1016/j.sbi.2006.10.001.
[27] Sniegowski, J.A., Lappe, J.W., Patel, H.N., Huffman, H.A., Wachter, R.M. 2005. Base Catalysis of Chromophore Formation in Arg96 and Glu222 Variants of Green Fluorescent Protein. J. Biol. Chem. 280: 26248–26255, http://dx.doi.org/10.1074/jbc.M41232720.
[28] Remington, S.J. 2011. Green fluorescent protein: A perspective. Protein Sci. 20(9): 1509–1519, http://dx.doi.org/10.1002/pro.684.
[29] Fu, J.L., Kanno, T., Liang, S.-C., Matzke, A.J.M., Matzke, M. 2015. GFP Loss-of-Function Mutations in Arabidopsis thaliana. Genes Genomes Genetics. 5(9): 1849–1855, http://dx.doi.org/10.1534/g3.115.019604.
[30] Stepanenko, O.V., Kuznetsova, I.M., Verkhusha, V.V., Turoverov, K.K. 2013. Beta-barrel scaffold of fluorescent proteins: folding, stability, and role in chromophore formation. Int. Rev. Cell. Mol. Biol. 302: 221–278, http://dx.doi.org/10.1016/B978-0-12-407699-0.00004-2.